

Journal of Pakistan Institute of Chemical Engineers



journal homepage: www.piche.org.pk/journal

DOI: https://doi.org/10.54693/piche.5212



Effect of Laser Scanning Speed on the Morphological Properties of CO₂ Laser Modified, Wire-arc Sprayed Aluminum Bronze Coatings, Deposited on Aisi-304 Stainless Steel

> A. Inam¹, M. Ishtiaq^{1,*}, A.M.H. Alvi¹, Misbah-ul-Hassan¹, Inam Ullah¹, H.M.R. Tariq² Submitted: 20/03/2024, Accepted: 31/05/2024, Published: 03/06/2024

Abstract

Herein, the effect of laser-scanning speeds on the morphological properties of CO_2 laser-modified, wire-arc sprayed aluminum bronze coating was investigated. Firstly, the aluminum bronze coating was deposited on AISI-304 stainless steel by wire-arc spray method. The surface of the deposited coating was then modified, using CO_2 laser remelting process under various scanning speeds, ranging from 100-500 mm/min. Scanning electron microscopy revealed that the CO_2 laser treatment melted the aluminum bronze coating and the substrate beneath. This melting resulted in a stable, homogeneous alloy of coating and substrate. At CO_2 laser scanning speed of 100 mm/min, the coating was deeply diffused into the substrate and formed a coating of 530.13 µm thickness, composed of an alloy coating and substrate. With the increase in CO_2 laser scanning speed, a gradual reduction in the thickness of the diffused coating was observed. At the maximum scanning speed of 500 mm/min, a 57% reduction in the diffused coating was observed, resulting in a thickness of 225.21 µm. SEM-EDS validated the diffusion of the aluminum bronze coating into the substrate by exhibiting 33.52 wt% Fe, 41.22 wt% Cu, and 2.39 wt% Al in the newly formed coating. With an increase in CO_2 laser scanning speed, the percentage of Fe was reduced whereas the percentage of Cu was increased in alloyed coatings. A maximum of $\sim 11\%$ reduction in Fe percentage and $\sim 18\%$ improvement in Cu percentage were achieved at the highest scanning speed of 500 mm/min, compared to 100 mm/min scanning speed.

Keywords: CO₂ Laser; Surface Lodification; Aluminum Bronze Coating; 304 Stainless Steel; Morphological Properties

1. Introduction:

Austenitic stainless steels are the most widely used ferrous materials in aerospace, biomedical, automobile, chemical, petrochemical, and food process industries because of their outstanding strength, toughness, and corrosion resistance [1]. The AISI–304 steel is one of the extensively used stainless steels in power plants, desalination

plants, hulls, submarines, ships, and pipelines due to their excellent corrosion and wear resistance with moderate mechanical properties [2-5]. The AISI-304 stainless steel possesses excellent corrosion resistance due to the presence of a chromium passive layer on the steel surface [6-9]. When this passive layer is damaged, the steel becomes vulnerable to harsh corrosion and wear

¹Institute of Metallurgy & Materials Engineering, University of the Punjab, 54590, Lahore, Pakistan ²Department of Mechanical Engineering, Incheon National University, Incheon, 22012, Republic of Korea Corresponding Author: ishtiaq.imme@pu.edu.pk

environments, which can lead to the failure of the steel component [9]. Therefore, it is mandatory to protect its surface from harsh conditions to extend its applications further by utilizing the application of proper protective coating [10, 11]. Various types of protective coatings, such as HVOF sprayed SiC-WC-Cr₃C₂ multilayer coatings [12], smart conducting polypyrrole coatings [13], ZrO₂-gelatin nanocomposites coatings [14], superhydrophobic coatings [15, 16], HVOF thermal sprayed NiAl coatings [17, 18], Ni₃S₂ coatings [19], TiO₂ coatings [19, 20], ethylaniline coatings [21], polyaniline coatings [22, 23], graphene coatings [24, 25], Ni coatings [26], Ni-Cr coatings [27], and many more [28-34] have been deposited on AISI-304 stainless steel surface.

The aluminum bronze alloys (Cu-Al-Fe) are known for having good wear properties and providing excellent resistance to corrosion in seawater [35]. Aluminum bronze can form layers of alumina (Al₂O₂ and cuprous oxide (Cu₂O) which provides excellent resistance to corrosion -[36]. The aluminum bronze alloy (Cu-Al-Fe) coatings demonstrate high hardness, excellent tensile strength, high corrosion, and wear resistance [37, 38], superior oxidation resistance at elevated temperatures, significant bondability, high deposition rate, and low cost [39, 40]. Although aluminum bronze coatings were applied on different substrates [37-40] there is no literature about the deposition of aluminum bronze coatings on AISI-304 stainless steel to the best of our knowledge.

All the above-mentioned properties are associated with the morphology and elemental composition of the coatings [41]. This implies that the aforementioned properties of aluminum bronze coatings can be further improved by modifying their morphology and elemental composition, which is possible through laser surface modification [42-44]. Laser surface modification (LSM) is a novel surface treatment process that involves rapid heating and partial melting of the surface of the materials. The cooling rate during solidification and solid phase

transformation determines the final morphology [43, 45-48]. Laser processes have been successfully applied before, during, or after coatings to improve the adhesion and mechanical properties of coatings [49]. Chen et al. deposited Ni-Cr-B-Si composite coatings on Ti6Al4V substrate and reported that microhardness increases by increasing laser scanning speed from 5 mm/sec to 20 mm/ sec [50]. However, there is no literature available on the effect of laser scanning speed on aluminum bronze coated AISI-304 stainless steel. Therefore, it was worth to study the surface modifications by laser, especially the effect of laser scanning speed on coating thickness.

For this purpose, aluminum bronze coatings were deposited on AISI-304 stainless steel substrate by wire arc spray deposition process. The aluminum bronze coatings were then modified by CO_2 laser under various scanning speeds, ranging from 100 to 500 mm/min. Scanning electron microscopy (SEM), and energy dispersive spectroscopy (EDS) was performed to evaluate the morphological properties of the modified coatings. The thickness of the modified coatings was also measured by SEM to elucidate the effect of laser scanning speed on coating thickness.

2. Experimental work:

2.1. Material:

The AISI-304 stainless steel was selected as a substrate material and obtained in the form of a sheet of 5 mm thickness. The chemical composition of the steel was determined by the optical emission spectrometer (MetaLab, Germany) as tabulated in Table 1. After the composition analysis, five samples of the AISI-304 stainless steel were wire cut into the dimensions of 3×1.5×5 mm and grit blasted by the alumina grits/particles of 5 µm size to attain a smooth and defect-free surface before deposition. The surface roughness of all samples was measured with a profilometer (Surfcorder SE1700a, USA) equipped with a 2 µm radius diamond tip, worked at 1 mm/sec speed for a 4 mm distance. For all samples, the average surface roughness of 5.5 µm was achieved after grit blasting.

С	Si	Mn	Ni	Cr	S	P	Fe
0.019	0.154	0.998	8.779	17.90	0.001	0.010	Balance

Table 1. Chemical composition of AISI-304 stainless steel used as a substrate (wt%).

Aluminum bronze alloy, having 89.5% Cu, 9.5% Al, and 1% Fe in chemical composition (wt%), was selected as a coating material and obtained in the form of SPRA-BRONZE—AA wires (Sulzer Metco, USA) of diameter 1.62 mm.

2.2 Wire-arc spray deposition process:

The aluminum bronze coatings were deposited on AISI-304 stainless steel substrate by the twin wire arc spray method. The aluminum bronze wires of diameter 1.62 mm were fed into the wire arc spraying system (*Sulzer Metco, USA*). The coating was sprayed on the substrate at a current/feed rate of 6.5 kW, spray distance of 4 inches, air pressure of 40 psi, and voltage of 30 V. The aluminum bronze coatings were deposited and cleaned for subsequent modification by CO₂ laser remelting process.

2.3. Coating modification by CO₂ laser remelting process:

To homogenize the surface and improve the surface properties of the deposited aluminum bronze coatings, a $\rm CO_2$ laser (NOVA pulse, 543CD-L, USA) was used for the remelting process. The surface modification of aluminum bronze coatings was made by applying the $\rm CO_2$ laser in continuous wave mode at a frequency of 10 Hz, wavelength of 532 nm, and energy of 150 MJ. The schematic of the $\rm CO_2$ laser modification process employed in this study is shown in Figure 1.

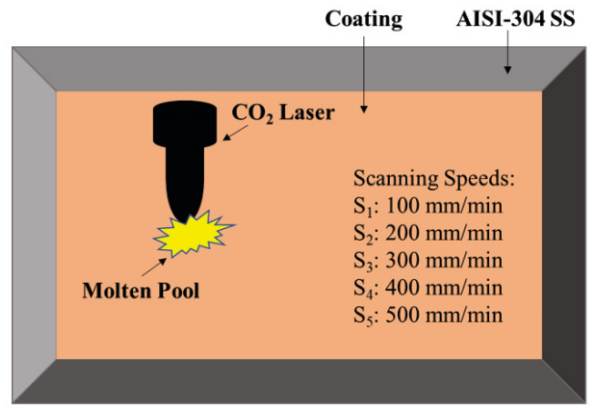


Figure.1. Schematic representation of laser modification process

Five beads of laser were drawn on the aluminum bronze coating at varying scanning speeds of 100, 200, 300, 400, and 500 mm/min as shown in Figure 2

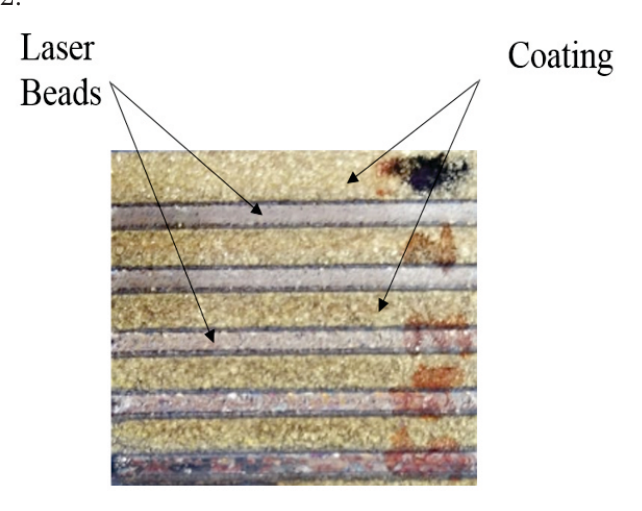


Figure 2: Surface modification of aluminum bronze coating with CO_2 laser remelting process, applied at various scanning speeds, ranging from 100 mm/min (bottom bead) to 500 mm/min (top bead).

2.4. Scanning electron microscopy:

To analyze the properties of original and laser-modified coatings, all the samples were metallographically prepared by manual grinding using standard practice and procedure on FEPA (Federation of European Producers of abrasives) grades P100, P200, P400, P600, P800, and P1000 grinding papers followed by automatic polishing on diamond pastes (6, 3, 1 and 0.25 μm) coated nylon and velvet cloths using an automatic polisher (StruersTegrapol-15 Grinder/Polisher, USA). Morphological examination of a cross-section of the ground and polished samples, comprising a substrate, coating, and the laser-modified zone, was carried out on an SEM (FEI brand Inspect S50, USA).

2.5. Energy dispersive spectroscopy:

To verify the coating deposition, elemental compositions, and elemental distribution of a cross-

section of the ground and polished samples, comprising a substrate, coating, and the laser-modified zone, an EDS, equipped with new generation silicon drift detector (SDD) attached with SEM, was used. For this purpose, the spot analysis technique was applied by selecting spots on modified coatings. To visualize the elemental distribution throughout the coated and modified substrate, the EDS mapping technique was also applied.

2.6 Thickness measurement:

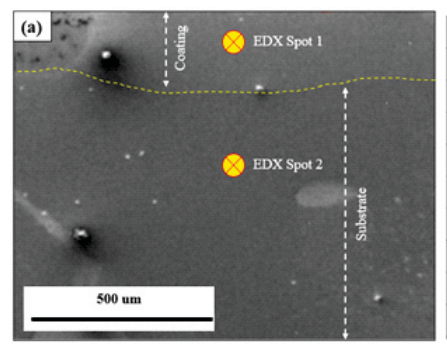
For the measurements of the thickness of coatings, the micrographs of cross-sections of the ground and polished samples, captured by SEM (*FEI brand model Inspect S50 USA*) were utilized. The coating thickness was measured by software (*Gatan Digital Micrograph*) on SEM images.

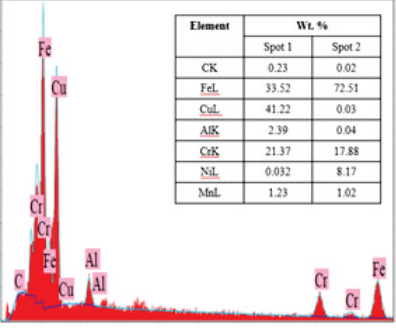
3. Results and discussion:

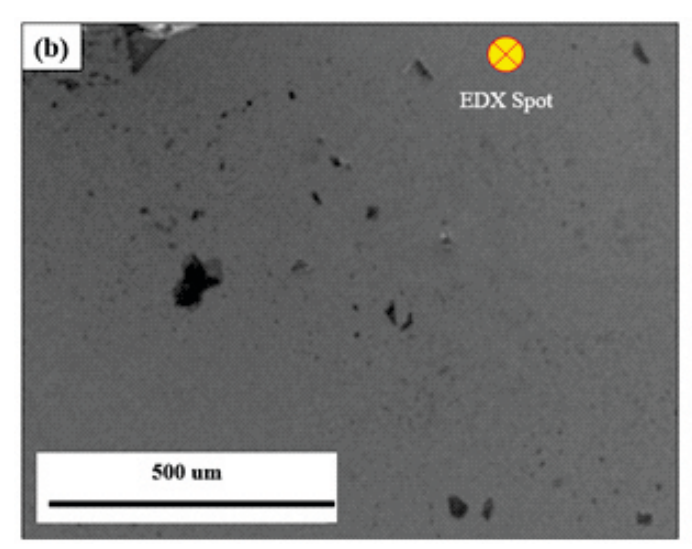
3.1. Morphological properties:

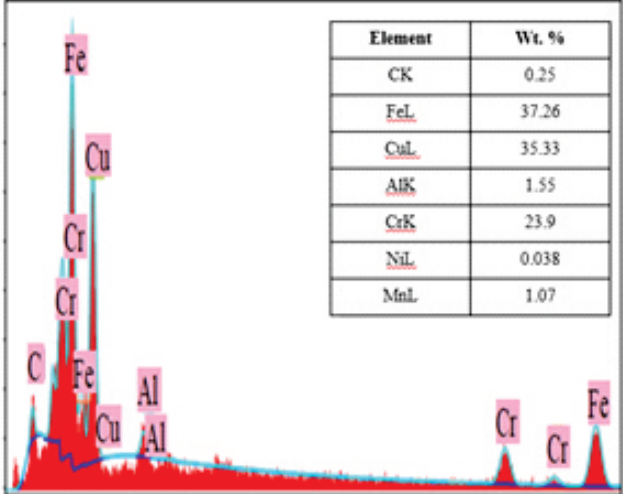
SEM images and EDS spectra of CO₂laser-modified aluminum bronze coating, deposited on AISI-304 stainless under various laser scanning speeds, ranging from 100-500 mm/min, are illustrated in Figure 3, whereas the corresponding SEM-EDS maps are presented in Figure 4. CO₂ laser beam properties, including coherence, polarization, angle of incidence to the target, and scanning speed, have a significant impact on the periodic energy absorption of the substrate, and resultant microstructure [51]. In general, the theory of microstructure formation after laser modification is very complicated and based on the Laser-Induced Periodic Surface Structure effect (LIPSS) [52, 53]. LIPSS effects are usually observed on metals, semiconductors, and other materials that have good absorbability of laser radiations and occur at low, medium, and high energy densities [54, 55]. In this

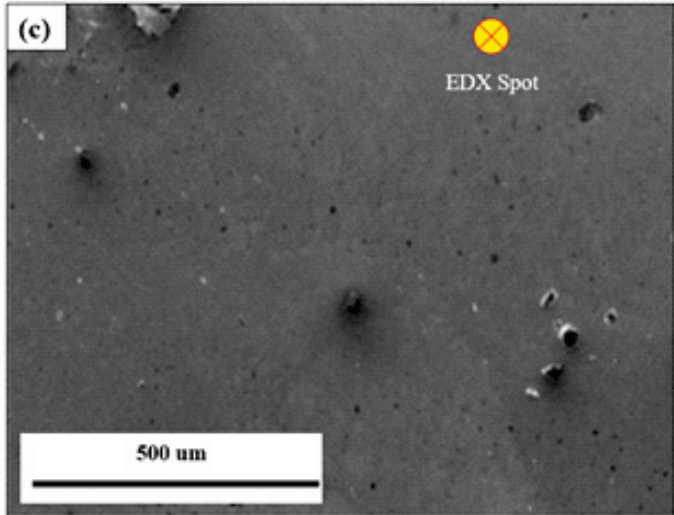
work, the SEM micrographs demonstrated the significant CO2 laser modification of aluminum bronze coating deposited on AISI-304 steel at all scanning speeds. SEM-EDS spectra validated the surface modification of aluminum bronze coating by exhibiting elemental mapping. The application of a CO₂ laser on the surface of aluminum bronze coated on AISI-304 stainless steel results in the melting of both the coating and the substrate, leading to the development of an alloyed coating on the substrate surface. Consequently, after CO₂ laser surface modification at a scanning speed of 100 mm/min, a significantly thicker, modified, and alloyed coating was obtained, as illustrated in Figure 3(a). SEM-EDS analysis was conducted on two spots: Spot 1, situated within the modified coating, confirmed the formation of the alloyed coating, with 33.52 wt% Fe, 41.22 wt% Cu, and 2.39 wt% Al, indicative of an aluminum bronze coating. Conversely, analysis at point 2, located within the substrate, revealed a composition of 72.51 wt% Fe, closely resembling the chemical composition of the examined sample. Furthermore, the increase in CO₂ laser scanning speed from 100 to 200 mm/min resulted in a relatively thinner coating with a slightly increased percentage of Fe (37.26 wt%) and a slightly decreased percentage of Cu (35.33 wt%) as depicted in Figure 3(b). This suggests a potential influence of scanning speed on the elemental composition and thickness of the alloyed coating. Further increase in scanning speeds to 300 and 400 mm/min led to a reduction in coating thickness and Fe percentage (35.68 wt%), while enhancing the Cu percentage (38.88 wt%, 38.85 wt%, respectively) as depicted in Figure 3(c, d). This trend is attributed to the reduced time for melting per unit area at higher scanning speeds, resulting in less melting of the substrate and more melting of the coating.

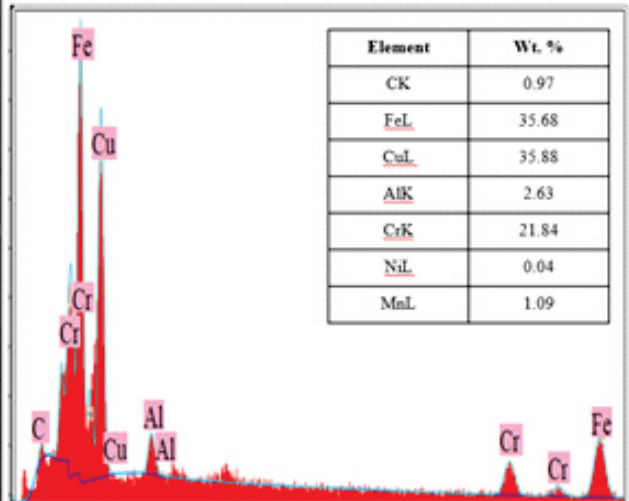


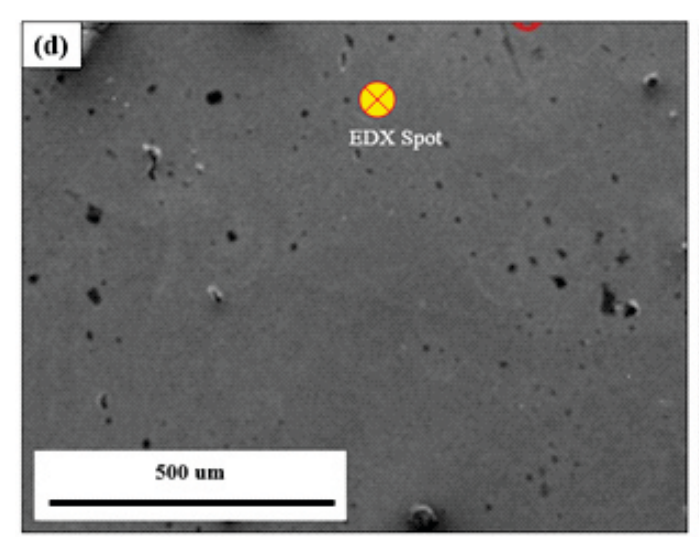


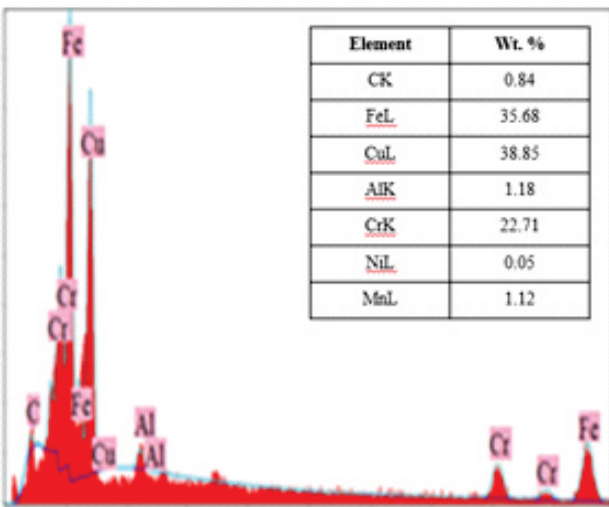












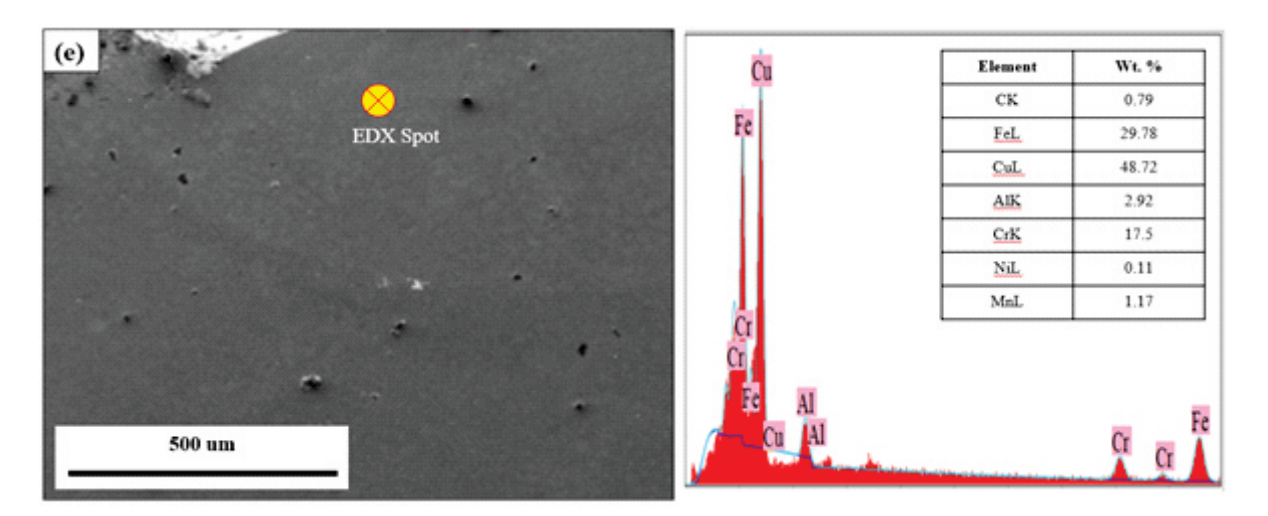


Figure 3: SEM spot EDS spectra of CO₂ laser-modified aluminum bronze coating, deposited on AISI-304 stainless steel at scanning speeds of (a) 100mm/min, (b) 200mm/min, (c) 300 mm/min (d) 400mm/min and (e) 500 mm/min

At a very fast scanning speed of 500 mm/min, the modification time per unit area was reduced further, causing the CO₂ laser to melt the coating to its maximum extent but failing to fully melt the substrate. This is corroborated by the data in Figure

3(e), which indicates the highest percentages of Cu (48.72 wt%) and Al (2.92 wt%), along with the lowest percentage of Fe (29.78 wt%). Consequently, the percentages of Cu and Al are relatively higher, while that of Fe is lower at this scanning speed.

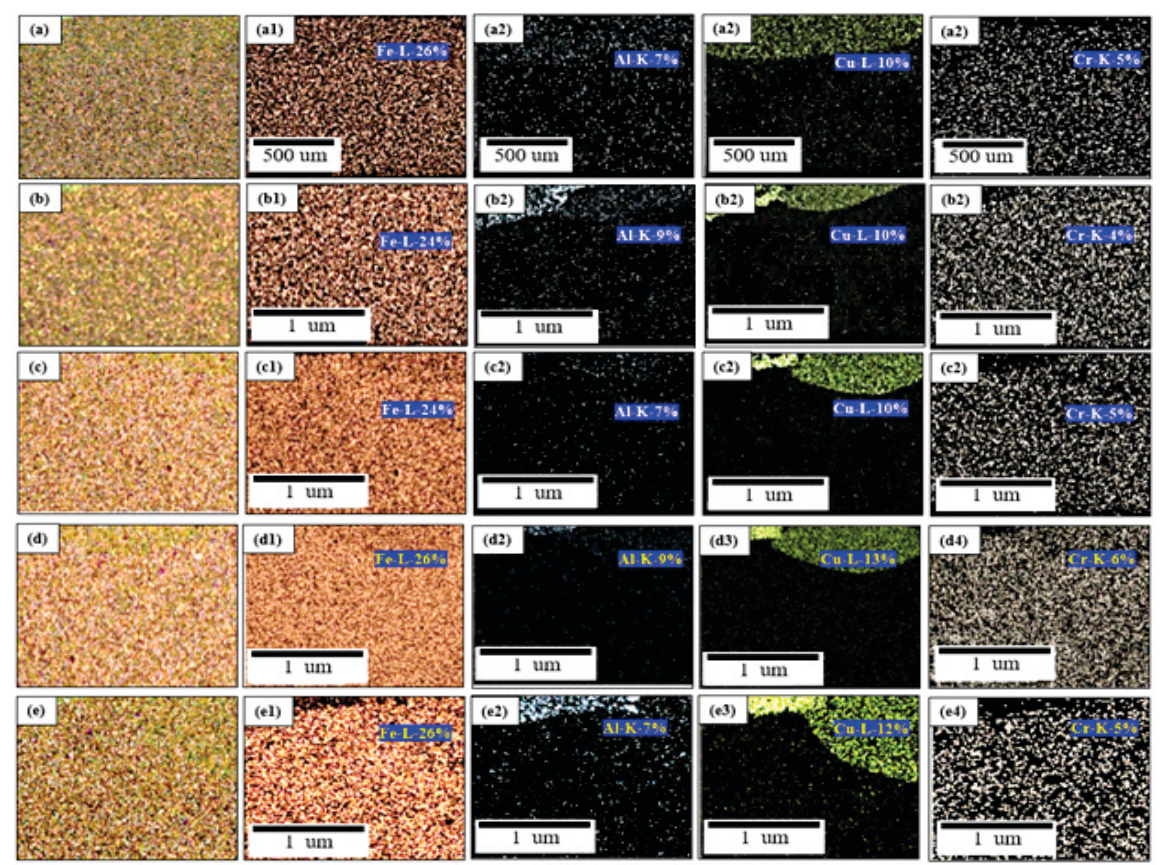


Figure 4: EDS maps of CO₂laser-modified aluminum bronze coatings, deposited on AISI-304 stainless steel at scanning speeds of (a) 100 mm/min (b) 200 mm/min (c) 300 mm/min (d) 400 mm/min (e) 500 mm/min.

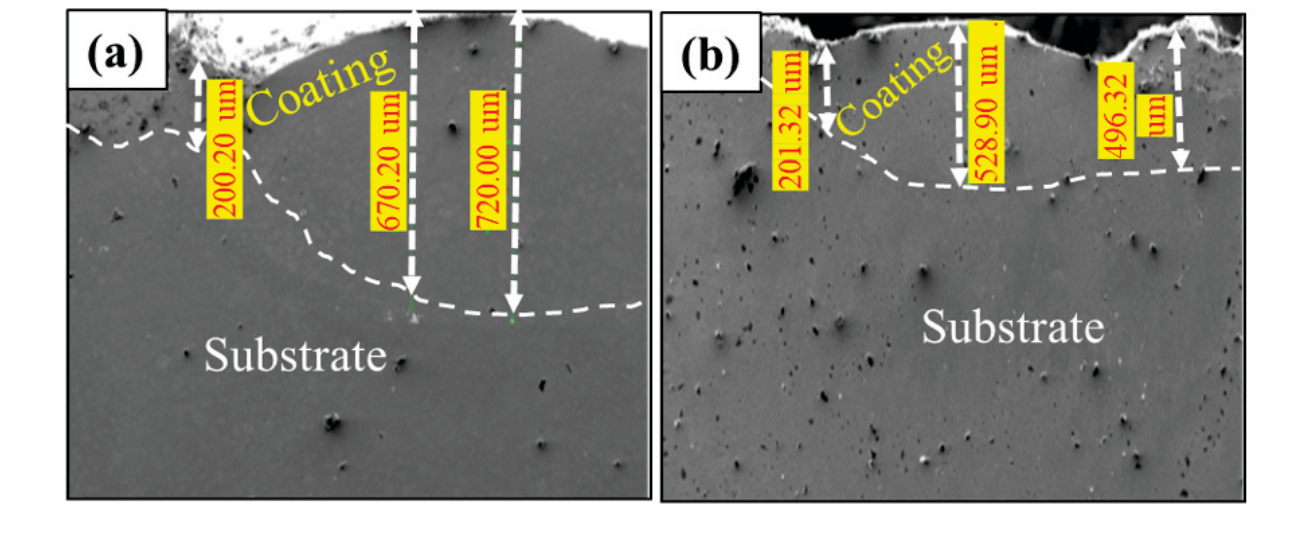
SEM-EDS elemental maps of CO₂ laser-modified aluminum bronze coating, deposited on AISI–304 stainless steel at various scanning speeds, ranging from 100 to 500 mm/min are illustrated in Figure 4. The results of SEM-EDS elemental maps are in good agreement with EDS spot analysis. At a scanning speed of 100 mm/min, SEM-EDS elemental maps exhibited 26 wt% Fe, 10 wt% Cu, 5 wt% Cr, and 7 wt% Al in the CO₂ laser-modified aluminum bronze coating. The overall composition of the coating showed all elements including Fe, Al, Cu, and Cr confirming the alloyed coating formation with the application of laser.

3.2 Coating thickness:

The influence of CO₂ laser scanning speed on the thickness of the aluminum bronze modified coating was found to be significant. To account for nonuniform coating thickness, measurements were taken from various areas and averaged. Crosssectional images of the coated samples were captured at five different locations along the length of each sample. At each location, thickness measurements were obtained at three equidistant points, resulting in a total of 15 measurements per sample. The average coating thickness was then calculated from these measurements. SEM micrographs used for thickness measurements of the aluminum bronze coatings are illustrated in Figure 5. Variations in average coating thickness values across different scanning speeds are

depicted in Figure 6. At a scanning speed of 100 mm/min, the aluminum bronze coating exhibited the highest average thickness of 530.13 μm , attributed to the slower scanning rate of the CO_2 laser. As the scanning speed increased, there was a gradual reduction in coating thickness. Specifically, the aluminum bronze coating deposited at 200 mm/min showed a 23% decrease in thickness (~408.85 μm) due to the slightly reduced time available for melting the coating and substrate compared to the coating deposited at 100 mm/min.

At moderate and relatively higher scanning speeds of 300 and 400 mm/min, considerable reductions in coating thickness were achieved, compared to the coating deposited at 100 mm/min. This is because, at relatively higher scanning speeds, the CO₂ laser found less time to melt the coating as well as the substrate. Therefore, relatively thinner coatings were produced at these scanning speeds. These results are in agreement with the previous findings about laser scanning speed reported somewhere else [56-58]. At a very fast scanning speed of 500 mm/min, a maximum 57% reduction in aluminum bronze coating thickness was observed, which is attributed to the very low available time for melting coating and substrate to produce an alloyed thicker coating.



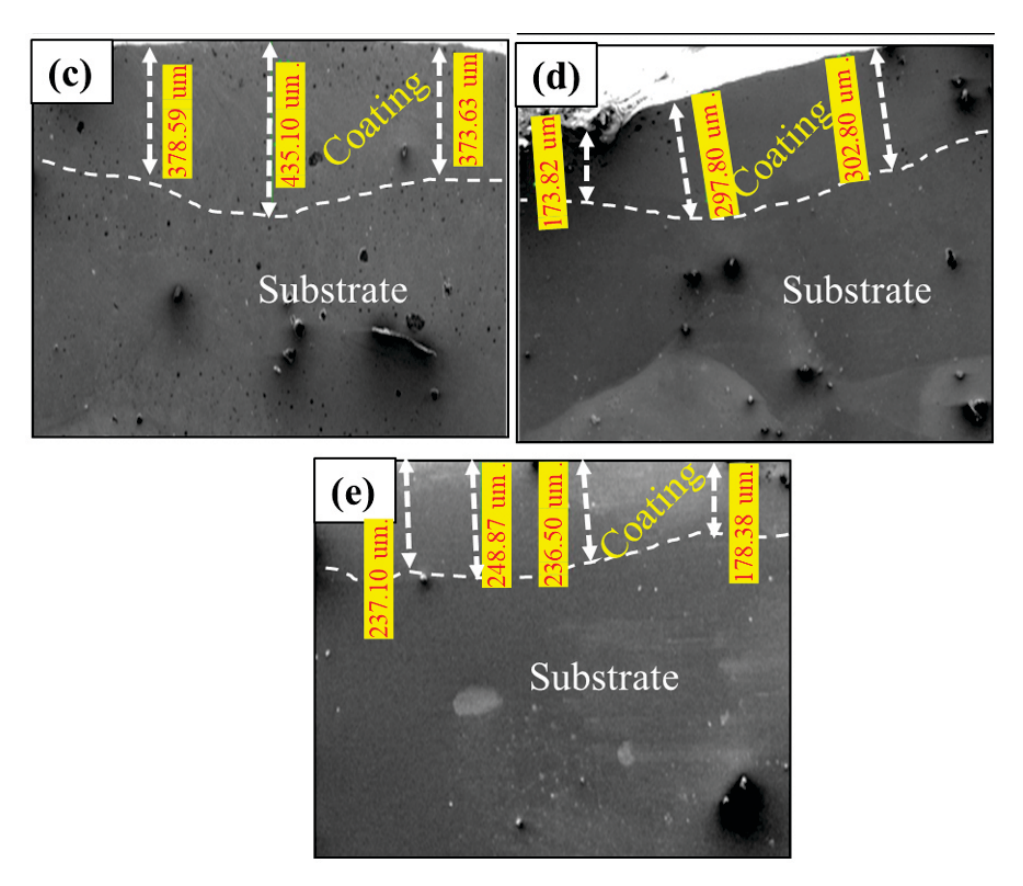


Figure 5: SEM images showing coating thickness of CO₂laser-modified aluminum bronze coatings, deposited on AISI-304 stainless steel at scanning speeds of (a) 100, (b) 200, (c) 300, (d) 400, and (e) 500 mm/min.

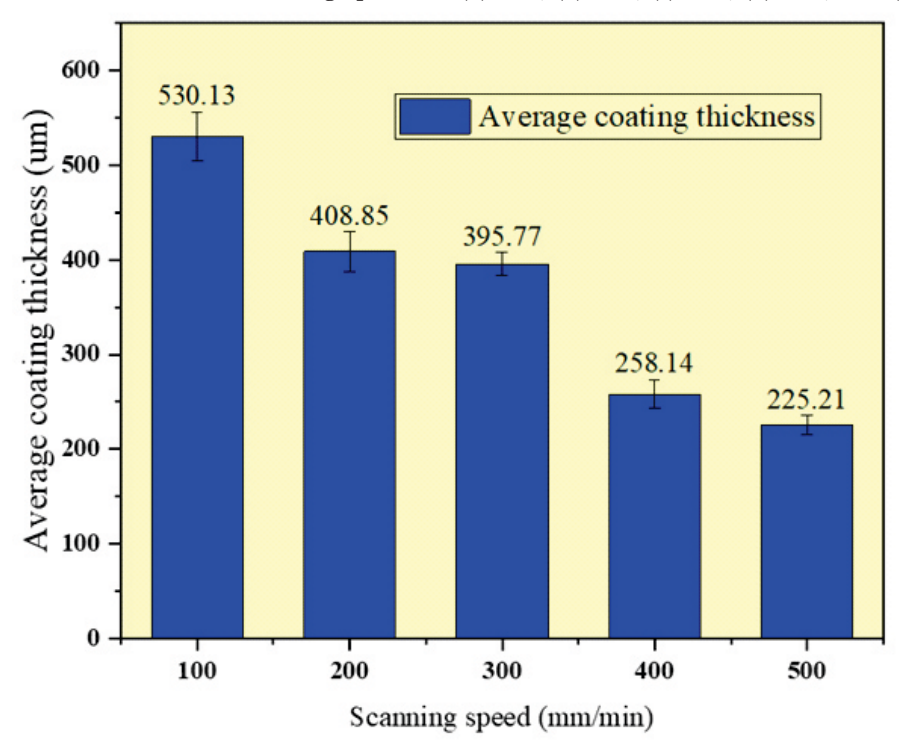


Figure 6: Variations in average coating thickness of CO₂ laser-modified aluminum bronze coating, deposited on AISI-304 stainless steel at various scanning speeds.

The relationship between laser scanning speed and average coating thickness is summarized in Figure 6. The data reveals a clear trend: as the scanning speed of the CO₂ laser increases, the average coating thickness decreases. For instance, at a scanning speed of 100 mm/min, the average coating thickness is 530.13µm, indicating a slower scanning rate results in a thicker coating. Conversely, at higher scanning speeds such as 200 mm/min, the average coating thickness decreases to 408.85 µm, signifying a reduction in thickness due to the increased speed of the laser scanning process. These findings provide valuable insights into the effect of scanning speed on the resulting coating thickness, which is essential for optimizing the laser surface modification process.

4. Conclusions:

From the present work, it can be concluded that the aluminum bronze coatings applied on AISI-304 stainless steel can be successfully modified to an alloyed coating having Fe, Al, Cu, and Cr. The CO₂ laser scanning speed exhibits an inverse relationship with the coating thickness i.e. thinner coating (225.21 um) is achieved at a higher scanning speed (500 mm/min), compared to a thicker coating (530.13 um) at a lower scanning speed (at 100 mm/min). These findings underscore the importance of controlling scanning parameters for tailored coating thicknesses in laser surface modification processes.

Conflict of Interest

The authors declare that they have no known competing financial interests or personal relationships that could have appeared to influence the work reported in this paper.

References:

- M. F. McGuire, "Austenitic Stainless Steels," in Encyclopedia of Materials: Science and Technology, K. H. J. Buschow et al., Eds. Oxford: Elsevier, 2001, pp. 406-410.
- 2. H. Wang et al., "Effect of martensitic phase transformation on the behavior of 304 austenitic stainless steel under tension," Materials Science and Engineering: A, vol. 649, pp. 174-183, 2016/01/01/2016.

- 3. J. Chen, R. M. Asmussen, D. Zagidulin, J. J. Noel, and D. W. Shoesmith, "Electrochemical and corrosion behavior of a 304 stainless-steel-based metal alloy wasteform in dilute aqueous environments," Corrosion Science, vol. 66, pp. 142-152, 2013.
- 4. G. F. Sun et al., "Microstructure and corrosion characteristics of 304 stainless steel laser-alloyed with CrCrB2," Applied Surface Science, vol. 295, pp. 94-107, 2014/03/15/2014.
- 5. J. Xu, X. Wu, and E.-H. Han, "Acoustic emission response of sensitized 304 stainless steel during intergranular corrosion and stress corrosion cracking," Corrosion Science, vol. 73, pp. 262-273, 2013.
- G. Lorang, M. Da Cunha Belo, A. M. P. Simões, and M. G. S. Ferreira, "Chemical Composition of Passive Films on AISI 304 Stainless Steel," Journal of The Electrochemical Society, vol. 141, no. 12, p. 3347, 1994/12/01 1994.
- L. R. Jordan, A. J. Betts, K. L. Dahm, P. A. Dearnley, and G. A. Wright, "Corrosion and passivation mechanism of chromium diboride coatings on stainless steel," Corrosion Science, vol. 47, no. 5, pp. 1085-1096, 2005/05/01/2005.
- 8. R. R. Ruf and C. C. Tsuei, "Extremely high corrosion resistance in amorphous Cr-B alloys," Journal of Applied Physics, Article vol. 54, no. 10, pp. 5705-5710, 1983.
- 9. R. W. Hertzberg and F. E. Hauser, "Deformation and fracture mechanics of engineering materials," 1977.
- 10. M. Li et al., "Microstructure and property of Ni/WC/La2O3 coatings by ultrasonic vibration-assisted laser cladding treatment," Optics and Lasers in Engineering, vol. 125, p. 105848, 2020/02/01/2020.
- 11. D. Guo, C. T. Kwok, and S. L. I. Chan, "Fabrication of stainless steel 316L/TiB2 composite coating via friction surfacing," Surface and Coatings Technology, vol. 350, pp. 936-948, 2018/09/25/2018.
- K. V. S. Rao, K. G. Girisha, K. Jamuna, and G.
 C. Tejaswini, "Erosion Behaviour of HVOF Sprayed SiC-WC-Cr3C2 Multilayer Coating on

- 304 Stainless Steel," Materials Today: Proceedings, vol. 5, no. 11, Part 3, pp. 24685-24690, 2018/01/01/2018.
- 13. Z. Chen, W. Yang, X. Yin, Y. Chen, Y. Liu, and B. Xu, "Corrosion protection of 304 stainless steel from a smart conducting polypyrrole coating doped with pH-sensitive molybdate-loaded TiO2 nanocontainers," Progress in Organic Coatings, vol. 146, p. 105750, 2020/09/01/2020.
- M. A. Almomani, M. T. Hayajneh, and M. Y. Al-Daraghmeh, "The corrosion behavior of AISI 304 stainless steel spin coated with ZrO2 gelatin nanocomposites," Materials Research Express, vol. 6, no. 9, p. 0965c4, 2019/07/31 2019.
- M. Pantoja, F. Velasco, J. Abenojar, and M. A. Martinez, "Development of superhydrophobic coatings on AISI 304 austenitic stainless steel with different surface pretreatments," Thin Solid Films, vol. 671, pp. 22-30, 2019/02/01/ 2019.
- 16. J. Bruzaud et al., "The design of superhydrophobic stainless steel surfaces by controlling nanostructures: a key parameter to reduce the implantation of pathogenic bacteria," Materials Science and Engineering: C, vol. 73, pp. 40-47, 2017.
- N. Abu-warda, A. J. López, M. D. López, and M. V. Utrilla, "High temperature corrosion and wear behavior of HVOF-sprayed coating of Al2O3-NiAl on AISI 304 stainless steel," Surface and Coatings Technology, vol. 359, pp. 35-46, 2019/02/15/2019.
- B. Wang and S. W. Lee, "Erosioncorrosion behaviour of HVOF NiAlAl2O3 intermetallicceramic coating," Wear, vol. 239, no. 1, pp. 83-90, 2000.
- Y. Nan et al., "Fabrication of Ni3S2/TiO2 photoanode material for 304 stainless steel photocathodic protection under visible light," Surface and Coatings Technology, vol. 377, p. 124935, 2019/11/15/2019.
- 20. Y. Ohko, S. Saitoh, T. Tatsuma, and A. Fujishima, "Photoelectrochemical

- anticorrosion and self-cleaning effects of a TiO2 coating for type 304 stainless steel," Journal of the Electrochemical Society, vol. 148, no. 1, p. B24, 2001.
- 21. A. Yağan, N. Özçiçek Pekmez, and A. Yıldız, "Poly(N-ethylaniline) coatings on 304 stainless steel for corrosion protection in aqueous HCl and NaCl solutions," Electrochimica Acta, vol. 53, no. 5, pp. 2474-2482, 2008/01/01/2008.
- 22. P. A. Kilmartin, L. Trier, and G. A. Wright, "Corrosion inhibition of polyaniline and poly(omethoxyaniline) on stainless steels," Synthetic Metals, vol. 131, no. 1, pp. 99-109, 2002/11/20/2002.
- 23. A. A. Hermas, M. Nakayama, and K. Ogura, "Enrichment of chromium-content in passive layers on stainless steel coated with polyaniline," Electrochimica Acta, vol. 50, no. 10, pp. 2001-2007, 2005/03/15/2005.
- 24. P. Mandal, N. Usha Kiran, U. K. Chanda, S. Pati, and S. Roy, "Corrosion performance of graphene oxide coated 304 SS in PEMFC environment," SN Applied Sciences, vol. 3, no. 7, p. 715, 2021/06/30 2021.
- 25. F. Abdi and H. Savaloni, "Corrosion Inhibition of AISI304 Stainless Steel by Graphen Oxide Coating," 01/01 2020.
- 26. V. Rajaei, H. Rashtchi, K. Raeissi, and M. Shamanian, "The study of Ni-based nanocrystalline and amorphous alloy coatings on AISI 304 stainless steel for PEM fuel cell bipolar plate application," International Journal of Hydrogen Energy, vol. 42, no. 20, pp. 14264-14278, 2017/05/18/2017.
- 27. J. Feng, M. G. S. Ferreira, and R. Vilar, "Laser cladding of Ni-Cr/Al2O3 composite coatings on AISI 304 stainless steel," Surface and Coatings Technology, vol. 88, no. 1, pp. 212-218, 1997/01/01/1997.
- 28. G. Zhang, H. Liu, X. Tian, P. Chen, H. Yang, and J. Hao, "Microstructure and Properties of AlCoCrFeNiSi High-Entropy Alloy Coating on AISI 304 Stainless Steel by Laser Cladding," Journal of Materials Engineering and Performance, vol. 29, no. 1, pp. 278-288,

- 2020/01/01 2020.
- C.-H. Hsu, K.-L. Chen, Z.-H. Lin, C.-Y. Su, and C.-K. Lin, "Bias effects on the tribological behavior of cathodic arc evaporated CrTiAlN coatings on AISI 304 stainless steel," Thin Solid Films, vol. 518, no. 14, pp. 3825-3829, 2010/05/03/2010.
- 30. M. Masanta, S. M. Shariff, and A. Roy Choudhury, "A comparative study of the tribological performances of laser clad TiB2TiCAl2O3 composite coatings on AISI 1020 and AISI 304 substrates," Wear, vol. 271, no. 7, pp. 1124-1133, 2011/07/18/2011.
- 31. L. Liu, Y. Qiao, and P. Xu, "Effect of La2O3 on Microstructure and Properties of Laser Cladding SMA Coating on AISI 304 Stainless Steel," Coatings, vol. 12, no. 7, p. 1004, 2022.
- 32. M. Atapour, V. Rajaei, S. Trasatti, M. P. Casaletto, and G. L. Chiarello, "Thin Niobium and Niobium Nitride PVD Coatings on AISI 304 Stainless Steel as Bipolar Plates for PEMFCs," Coatings, vol. 10, no. 9, p. 889, 2020.
- 33 J.-H. Huang, Z.-E. Tsai, and G.-P. Yu, "Mechanical properties and corrosion resistance of nanocrystalline ZrNxOy coatings on AISI 304 stainless steel by ion plating," Surface and Coatings Technology, vol. 202, no. 20, pp. 4992-5000, 2008/07/15/2008.
- 34. G. Singh, H. Singh, and B. S. Sidhu, "Corrosion behavior of plasma sprayed hydroxyapatite and hydroxyapatite-silicon oxide coatings on AISI 304 for biomedical application," Applied Surface Science, vol. 284, pp. 811-818, 2013/11/01/2013.
- 35. A. H. Tuthill, Guidelines for the use of copper alloys in seawater. Nickel Development Institute, 1987.
- 36. A. Schüssler and H. Exner, "The corrosion of nickel-aluminium bronzes in seawaterI. Protective layer formation and the passivation mechanism," Corrosion Science, vol. 34, no. 11, pp. 1793-1802, 1993.
- 37. S. Alam, S. Sasaki, and H. Shimura, "Friction and wear characteristics of aluminum bronze coatings on steel substrates sprayed by a low

- pressure plasma technique," Wear, vol. 248, no. 1, pp. 75-81, 2001/03/01/2001.
- 38. W. Liang, X. Xiaolei, X. Jiujun, and H. Zukun, "Microstructures and properties of PVD aluminum bronze coatings," Thin Solid Films, vol. 376, no. 1, pp. 159-163, 2000/11/01/2000.
- 39. Z.-l. Zhang, D.-y. Li, and S.-y. Wang, "High temperature performance of arc-sprayed aluminum bronze coatings for steel," Transactions of Nonferrous Metals Society of China, vol. 16, no. 4, pp. 868-872, 2006/08/01/2006.
- 40. X. P. Tao, S. Zhang, C. H. Zhang, C. L. Wu, J. Chen, and A. O. Abdullah, "Effect of Fe and Ni contents on microstructure and wear resistance of aluminum bronze coatings on 316 stainless steel by laser cladding," Surface and Coatings Technology, vol. 342, pp. 76-84, 2018/05/25/2018.
- 41. J. Zhou, M. Yang, R. Wang, and X. Pang, "Annealing behavior of aluminum coating prepared by arc spraying on P355NL1 steel," Surface and Coatings Technology, vol. 330, pp. 53-60, 2017/12/01/2017.
- 42. R. Krishnan, S. Dash, R. Kesavamoorthy, C. Babu Rao, A. K. Tyagi, and B. Raj, "Laser surface modification and characterization of air plasma sprayed alumina coatings," Surface and Coatings Technology, vol. 200, no. 8, pp. 2791-2799, 2006/01/24/2006.
- 43. R. Ahmadi-Pidani, R. Shoja-Razavi, R. Mozafarinia, and H. Jamali, "Improving the thermal shock resistance of plasma sprayed CYSZ thermal barrier coatings by laser surface modification," Optics and Lasers in Engineering, vol. 50, no. 5, pp. 780-786, 2012/05/01/2012.
- 44. R. Ahmadi-Pidani, R. Shoja-Razavi, R. Mozafarinia, and H. Jamali, "Laser surface modification of plasma sprayed CYSZ thermal barrier coatings," Ceramics International, vol. 39, no. 3, pp. 2473-2480, 2013/04/01/2013.
- 45. P.-C. Tsai, J.-H. Lee, and C.-L. Chang, "Improving the erosion resistance of plasmasprayed zirconia thermal barrier coatings by

- laser glazing," Surface and Coatings Technology, vol. 202, no. 4, pp. 719-724, 2007/12/15/2007.
- X. Wang, P. Xiao, M. Schmidt, and L. Li, "Laser processing of yttria stabilised zirconia/alumina coatings on Fecralloy substrates," Surface and Coatings Technology, vol. 187, no. 2, pp. 370-376, 2004/10/22/2004.
- 47. H. Chen, Y. Hao, H. Wang, and W. Tang, "Analysis of the microstructure and thermal shock resistance of laser glazed nanostructured zirconia TBCs," Journal of thermal spray technology, vol. 19, no. 3, pp. 558-565, 2010.
- 48. M. Morks, C. Berndt, Y. Durandet, M. Brandt, and J. Wang, "Microscopic observation of laser glazed yttria-stabilized zirconia coatings," Applied Surface Science, vol. 256, no. 21, pp. 6213-6218, 2010.
- 49. D. Garcia-Alonso, N. Serres, C. Demian, S. Costil, C. Langlade, and C. Coddet, "Pre-/During-/Post-Laser Processes to Enhance the Adhesion and Mechanical Properties of Thermal-Sprayed Coatings with a Reduced Environmental Impact," Journal of Thermal Spray Technology, vol. 20, no. 4, pp. 719-735, 2011/06/01 2011.
- 50. J. Chen, J. Li, R. Song, L. Bai, J. Shao, and C. Qu, "Effect of the scanning speed on microstructural evolution and wear behaviors of laser cladding NiCrBSi composite coatings," Optics & Laser Technology, vol. 72, pp. 86-99, 2015.
- 51. M. S. Trtica et al., "Surface modifications of TiN coating by the pulsed TEA CO2 and KrCl laser," Applied Surface Science, vol. 225, no. 1, pp. 362-371, 2004/03/30/2004.
- 52. J. F. Young, J. E. Sipe, and H. M. van Driel, "Laser-induced periodic surface structure. III. Fluence regimes, the role of feedback, and details of the induced topography in germanium," Physical Review B, vol. 30, no. 4, pp. 2001-2015, 08/15/1984.
- 53. J. E. Sipe, J. F. Young, J. S. Preston, and H. M. van Driel, "Laser-induced periodic surface

- structure. I. Theory," Physical Review B, vol. 27, no. 2, pp. 1141-1154, 01/15/1983.
- 54. J. F. Young, J. S. Preston, H. M. van Driel, and J. E. Sipe, "Laser-induced periodic surface structure. II. Experiments on Ge, Si, Al, and brass," Physical Review B, vol. 27, no. 2, pp. 1155-1172, 01/15/1983.
- 55. H. M. van Driel, J. E. Sipe, and J. F. Young, "Laser-Induced Periodic Surface Structure on Solids: A Universal Phenomenon," Physical Review Letters, vol. 49, no. 26, pp. 1955-1958, 12/27/1982.
- 56. X. Li et al., "Manufacturing of Ti3SiC2 lubricated Co-based alloy coatings using laser cladding technology," Optics & Laser Technology, vol. 114, pp. 209-215, 2019.
- 57. K. Zhang, S. Wang, W. Liu, and X. Shang, "Characterization of stainless steel parts by laser metal deposition shaping," Materials & Design, vol. 55, pp. 104-119, 2014.
- 58. X. Jiao, J. Wang, C. Wang, Z. Gong, X. Pang, and S. Xiong, "Effect of laser scanning speed on microstructure and wear properties of T15M cladding coating fabricated by laser cladding technology," Optics and Lasers in Engineering, vol. 110, pp. 163-171, 2018.